



Soft Matter

**Formation and Properties of Liposome-Stabilized All-Aqueous Emulsions Based on PEG/Dextran, PEG/Ficoll, and PEG/Sulfate Aqueous Biphasic Systems**

Journal:	<i>Soft Matter</i>
Manuscript ID	SM-ART-10-2020-001849.R1
Article Type:	Paper
Date Submitted by the Author:	16-Feb-2021
Complete List of Authors:	Rowland, Andrew; Penn State University Park, Chemistry Keating, Christine; Penn State University Park, Department of Chemistry

SCHOLARONE™  
Manuscripts

## Formation and Properties of Liposome-Stabilized All-Aqueous Emulsions Based on PEG/Dextran, PEG/Ficoll, and PEG/Sulfate Aqueous Biphasic Systems

Andrew T. Rowland and Christine D. Keating\*

*Department of Chemistry, Pennsylvania State University, University Park, Pennsylvania 16802,*

*USA.*

*E-mail: keating@chem.psu.edu*

### Abstract

Vesicle-stabilized all-aqueous emulsion droplets are appealing as bioreactors because they provide uniform encapsulation via equilibrium partitioning without restricting diffusion in and out of the interior. These properties rely on the composition of the aqueous two-phase system (ATPS) chosen for the emulsion and the structure of the interfacial liposome layer, respectively. Here, we explore how changing the aqueous two-phase system from a standard poly(ethyleneglycol), PEG, 8kDa/dextran 10kDa ATPS to PEG 8kDa /Ficoll 70kDa or PEG 8kDa/Na<sub>2</sub>SO<sub>4</sub> systems impacts droplet uniformity and partitioning of a model solute (U15 oligoRNA). We also compare liposomes formed by two different methods, both of which begin with multilamellar, polydisperse vesicles formed by gentle hydration: (1) extrusion, which produced vesicles of 150 nm average diameter, and (2) vortexing, which produced vesicles of 270 nm average diameter. Our data illustrate that while droplet uniformity and stability are somewhat better for samples based on extruded vesicles, extrusion is not necessary to create functional microreactors, as emulsions stabilized with vortexed liposomes are just as effective at

solute partitioning and allow diffusion across the droplet's liposome corona. This work expands the compositions possible for liposome-stabilized, all-aqueous emulsion droplet bioreactors, making them amenable to a wider range of potential reactions. Replacing the liposome extrusion step with vortexing can reduce time and cost of bioreactor production with only modest reductions in emulsion quality.

## **Introduction**

Stabilized emulsions have recently received considerable attention as artificial cells<sup>1-2</sup> and microscale reactors.<sup>3-6</sup> Droplets of a dispersed phase are suspended in a continuous phase, which comprise the reactor interior and exterior, respectively. Reactor loading is based on equilibrium partitioning between the two phases, providing homogeneous catalyst and reagent loading across the droplet population. Although oil/water-based systems are traditional, all-aqueous emulsions are appealing for bioreactors and artificial cell systems where it is beneficial for both the dispersed and continuous phases to be biocompatible. One form of aqueous liquid-liquid phase separation, coacervation, results from macromolecular associative interactions to form dense, polymer-rich droplets within a dilute phase.<sup>7-9</sup> These coacervate droplets have been utilized as biocompatible micro-reactors.<sup>10-12</sup> In contrast, non-associative (or segregative) liquid-liquid phase separation generates phases that are enriched in different components, e.g. different uncharged polymers or one polymer and salt. Without the strong associative interactions found in coacervate systems, relative phase volumes, viscosities, and compositions can be more similar to each other, simplifying phase manipulation (e.g., via pipetting) and characterization (due to sufficient volume of each phase to, e.g., fill a cuvette). These non-associative aqueous two-phase systems (ATPS) have long been of interest in bioseparations, commonly used for extraction and

purification of molecules or bioparticulates (e.g. chloroplasts).<sup>13-17</sup> More recently, ATPS have also been considered as biomimetic media.<sup>18-22</sup> Their macromolecular-rich phases resemble crowded biological fluids such as the cytoplasm, which can be upwards of 30% biomacromolecules by volume.<sup>23</sup> Macromolecular crowding has been shown to have a significant effect on biomolecular interactions and reactions, and should be considered when designing bioinspired environments.<sup>23-24</sup> ATPS also provide coexisting compartments with differing chemical and physical properties. Droplet loading with cargo such as enzymes is driven by preferential partitioning between the two phases, which is dictated by the phase compositions and has been well-studied for bulk poly(ethyleneglycol) PEG/dextran (Dx) and PEG/salt ATPS.<sup>25-26</sup>

ATPS emulsions can be produced by dispersing one aqueous phase within the other. Interfacial stabilization is necessary to inhibit coalescence of the dispersed phase droplets. The Pickering effect, whereby solid particles adsorb to the emulsion interface, has been used to stabilize all-aqueous emulsions.<sup>27-28</sup> These so-called Pickering emulsions have been prepared using a variety of particle materials, including protein nanoparticles,<sup>29-30</sup> silica nanoparticles,<sup>31</sup> and cellulose particles.<sup>32-33</sup> Others have formed polyelectrolyte assemblies at the droplet interfaces to serve as permeable membranes around individual droplets.<sup>34-35</sup> We previously reported reactive all-aqueous emulsions based on PEG/Dx ATPS stabilized with lipid vesicles of ~130 nm in diameter. The vesicles, which were negatively charged and produced by extrusion in PEG-rich phase, formed a submonolayer at the aqueous/aqueous interface to create Pickering-like emulsions.<sup>36</sup> Reactions such as RNA cleavage and CaCO<sub>3</sub> mineralization could be performed in these systems, although increased solution ionic strength was found to compromise droplet stability by reducing the electrostatic repulsion between vesicle-decorated droplets.<sup>37-38</sup>

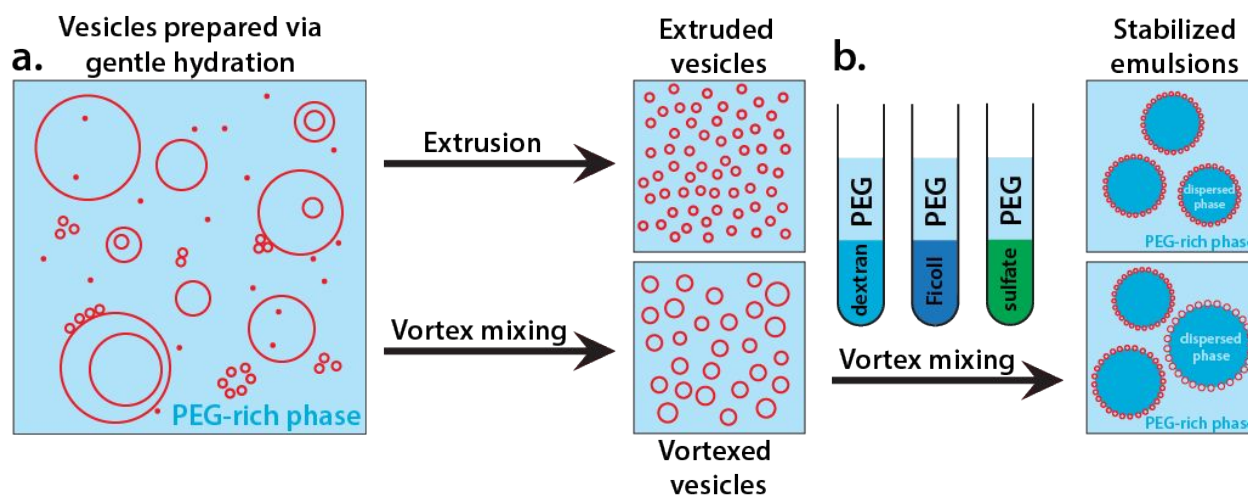
Nearly all prior examples of emulsion-based microreactors were based on the PEG/dextran ATPS.<sup>32-38</sup> By changing the ATPS composition, though, one could potentially alter the solvent properties and solute partitioning. This would be advantageous to expanding the breadth of reaction types in these liposome-stabilized micro-reactors. For instance, certain biocatalysts such as amylase and acylase function more effectively in the salt-rich phase of polymer/salt ATPS.<sup>39-40</sup> We have also demonstrated enhanced horseradish peroxidase activity in the salt-rich in contrast to the associated PEG-rich phase.<sup>41</sup> In this paper, PEG/Ficoll and PEG/sulfate ATPS were investigated as potential bases for liposome-stabilized emulsion. The influence of extrusion of liposomes on the efficacy of these systems was also investigated. Various stabilized ATPS emulsions were prepared using liposomes with identical lipid compositions that were either extruded or vortexed, characterized based on their short-term stability, permeability to solutes, and ability to encapsulate reactions.

## **Results**

### **Formation of stabilized all aqueous emulsions**

The general approach to producing all-aqueous emulsions was: (1) prepare initial lipid vesicles in a medium osmotically-matched to the intended final solution, (2) reduce average vesicle size by one of two treatment methods, and (3) combine with desired ATPS to produce liposome-stabilized all aqueous emulsions (see Scheme 1). We used lipid combinations having an equal mole fraction of zwitterionic phosphatidylcholine and anionic phosphatidylglycerol headgroups, with 2.8 mol % 2 kDa PEGylated lipid. The choice of lipids having PEGylated headgroups and negatively charged headgroups was made to reduce liposome solubility in both phases, to favor interfacial adsorption.<sup>36</sup> Liposomes were prepared in PEG-rich phase, or PEG

solution for PEG/sulfate ATPS samples, using the gentle hydration method.<sup>36, 42</sup> The resulting liposomes were a heterogeneous mixture of uni- and multilamellar vesicles as well as lipid aggregates. Dynamic light scattering (DLS) analysis of our gentle hydration raw product revealed an average particle diameter of  $3200 \pm 200$  nm. This material was then either extruded through polycarbonate membranes with 200 nm pores (“extruded”) or placed on the vortex mixer for  $\sim 10$  seconds (“vortexed”). The extrusion process narrowed the liposome size distribution, reducing the average diameter to  $154 \pm 4$  nm. Vortex mixing also narrowed the size distribution, albeit to a lesser extent, with post-vortexing average liposome diameters of  $270 \pm 20$  nm. Vortex mixing has been suggested as an alternative to sonication or extrusion in case of encapsulating more sensitive materials such as DNA or RNA.<sup>43</sup>



**Scheme 1: Schematic representation of the preparation of liposome-stabilized emulsions.** (a) Vesicles prepared via the gentle hydration are homogenized using either extrusion or vortex mixing. (b) Homogenized vesicles are added to one of three bulk ATPS then vortex mixed to form stabilized emulsions.

In order to test the flexibility of liposomes as stabilizers, three different ATPS were studied, each composed of water, polyethylene glycol (PEG 8 kDa), and a second polymer or a salt. The three compositions tested were PEG and dextran (Dx, 10 kDa), PEG and Ficoll (70 kDa), and PEG and sulfate (as  $\text{Na}_2\text{SO}_4^{2-}$ ). Individual phases were allowed to equilibrate and then

separated and recombined for a relative phase volume of 1:9, where the PEG-rich phase was chosen to be the larger volume phase;<sup>44</sup> this ensured that the PEG-rich phase was the continuous phase, and the droplets (distributed phase) had different major components depending on which system was under study (e.g., Dx-rich phase, or Ficoll-rich phase, or sulfate-rich phase).

Extruded or vortexed lipid vesicles were suspended in the PEG-rich phase portions at this stage, with the added volume of liposomes in PEG-rich phases included in the ratio. Mechanical agitation resulted in suspensions of droplets of the smaller-volume phase in the larger, continuous PEG-rich phase (see final panel of Scheme 1). In all cases, regardless of liposome treatment or ATPS composition, we found that the vesicles accumulated at the aqueous/aqueous interfaces between the two phases (Figure 1).

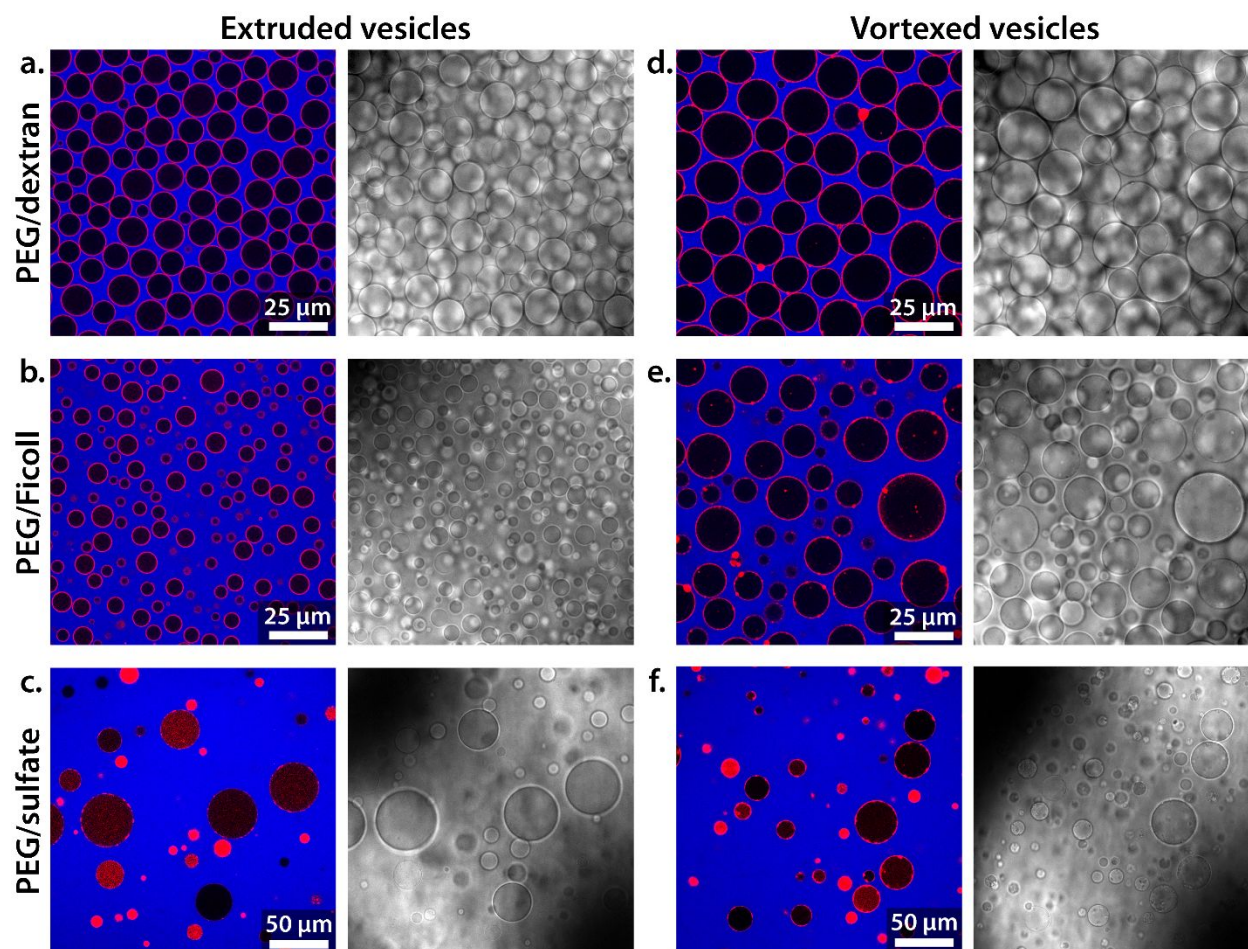


**Figure 1: Effect of ATPS identity and lipid vesicle preparation method on appearance of vesicle-stabilized all-aqueous emulsions.** Fluorescent confocal microscopy images of various aqueous two-phase separation (ATPS) emulsions stabilized with extruded (**a, b, c**) and vortexed (**d, e, f**) liposomes. Vortexed liposomes were able to effectively stabilize droplets of one phase within a continuous PEG-rich phase in the same manner as extruded liposomes with identical lipid composition. (**a,d**) PEG/dextran emulsions; (**b,e**) PEG/Ficoll emulsions; (**c,f**) PEG/sulfate emulsions. All images were acquired within ~15 minutes of sample preparation. Left panels = overlaid fluorescence; right panels = brightfield. Rhodamine-labeled vesicles have been false colored red, Alexa 647-tagged PEG has been false colored blue.

### **Influence of extrusion on emulsion size distribution**

Comparing the two liposome treatments in Figure 1, it appears that average droplet sizes are larger for ATPS stabilized using vortexed vs extruded vesicles for PEG/Dx and PEG/Ficoll ATPS emulsions. This is consistent with the larger average size of the vortexed vesicles themselves, reducing the area of interface that could be stabilized. The heterogeneity in droplet size apparent for the PEG/sulfate ATPS emulsions suggests a less stable emulsion, perhaps due to less effective interfacial assembly of vesicles under the high ionic strength solution conditions in this ATPS; several droplets show high vesicle encapsulation in the salt-rich phase. Figure 2 shows quantification of droplet size for the six conditions. Extrusion of vesicles reduces the average vesicle-stabilized dextran-rich phase droplet diameter from  $13 \pm 2$  to  $7 \pm 1$   $\mu\text{m}$  (Figure 2a). Likewise, the average Ficoll-rich diameter reduced from  $9 \pm 3$   $\mu\text{m}$  to  $5 \pm 1$   $\mu\text{m}$  (Figure 2b). The stabilized sulfate-rich droplets are relatively larger and more variable in size than those of the other ATPSs and were insensitive to replacing extruded vesicles with vortexed vesicles (average droplets diameters  $10 \pm 4$  vs  $9 \pm 4$   $\mu\text{m}$ ) (Figure 2c).



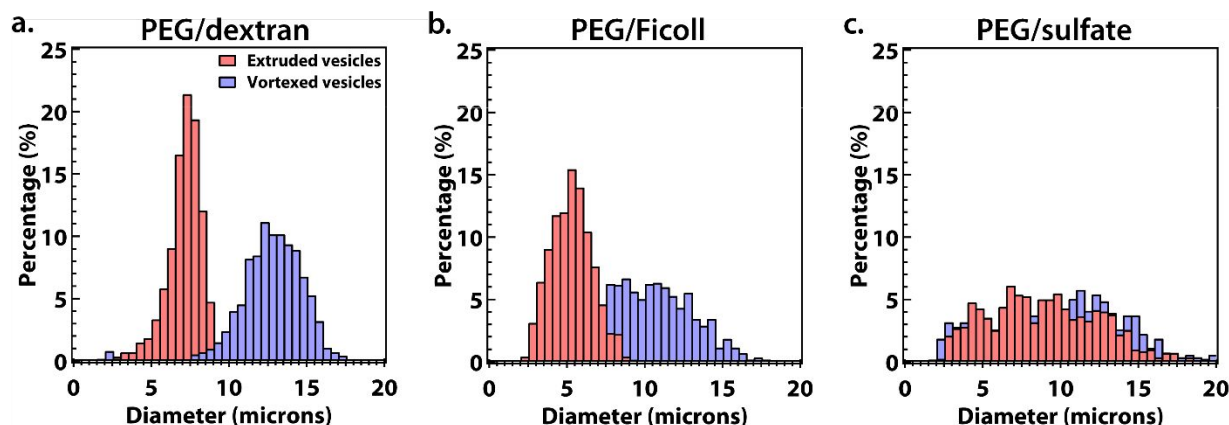


**Figure 2: Effect of ATPS identity and lipid vesicle preparation method on size distributions of vesicle-stabilized all-aqueous emulsions.** Size histograms of droplets in extruded and vortexed vesicle stabilized ATPS emulsions. In general, vesicle extrusion results in a decrease in average droplet diameter and distribution. **(a)** Measurements of vesicle (extruded and vortexed)-stabilized dextran-rich droplets; **(b)** measurements of vesicle-stabilized Ficoll-rich droplets; **(c)** measurements of vesicle-stabilized sulfate-rich droplets. Red bars indicate emulsions with extruded vesicles, blue indicate vortexed. Approximately 1200 droplets were measured across 4 to 5 images for each data set.

### Examination of emulsion short-term stability

The short-term stability of the liposome containing emulsions was tested by allowing the original samples to equilibrate for 24 hours on the coverslip (Figure 3). A similar experiment was performed for longer times, where samples sat for 5 days (Figure S1). Larger average droplet sizes observed for samples aged for 24 hours indicated that some coalescence had occurred in all samples (Figure S2). Increased Rhodamine fluorescence can be observed in the dispersed phases, particularly in the Ficoll and sulfate containing samples (Figure 3 b, c). We interpret this increased fluorescence as indicating higher concentration of free vesicles in the sulfate-rich (or Ficoll-rich) interior phases as droplet coalescence reduces the available surface area in the samples. After 5 days, significantly larger droplets were observed, indicating further coalescence; these larger droplets maintained a vesicle coating. The PEG/dextran samples showed the least amount of coalescence whereas the PEG/sulfate showed the greatest. These observations are in line with the sample appearance after their initial appearance; the fresh

dextran/PEG emulsions appear the most stable, with fairly homogeneous size distributions of dextran droplets. Inversely, the sulfate droplets appear the least stable for the opposite reasons.

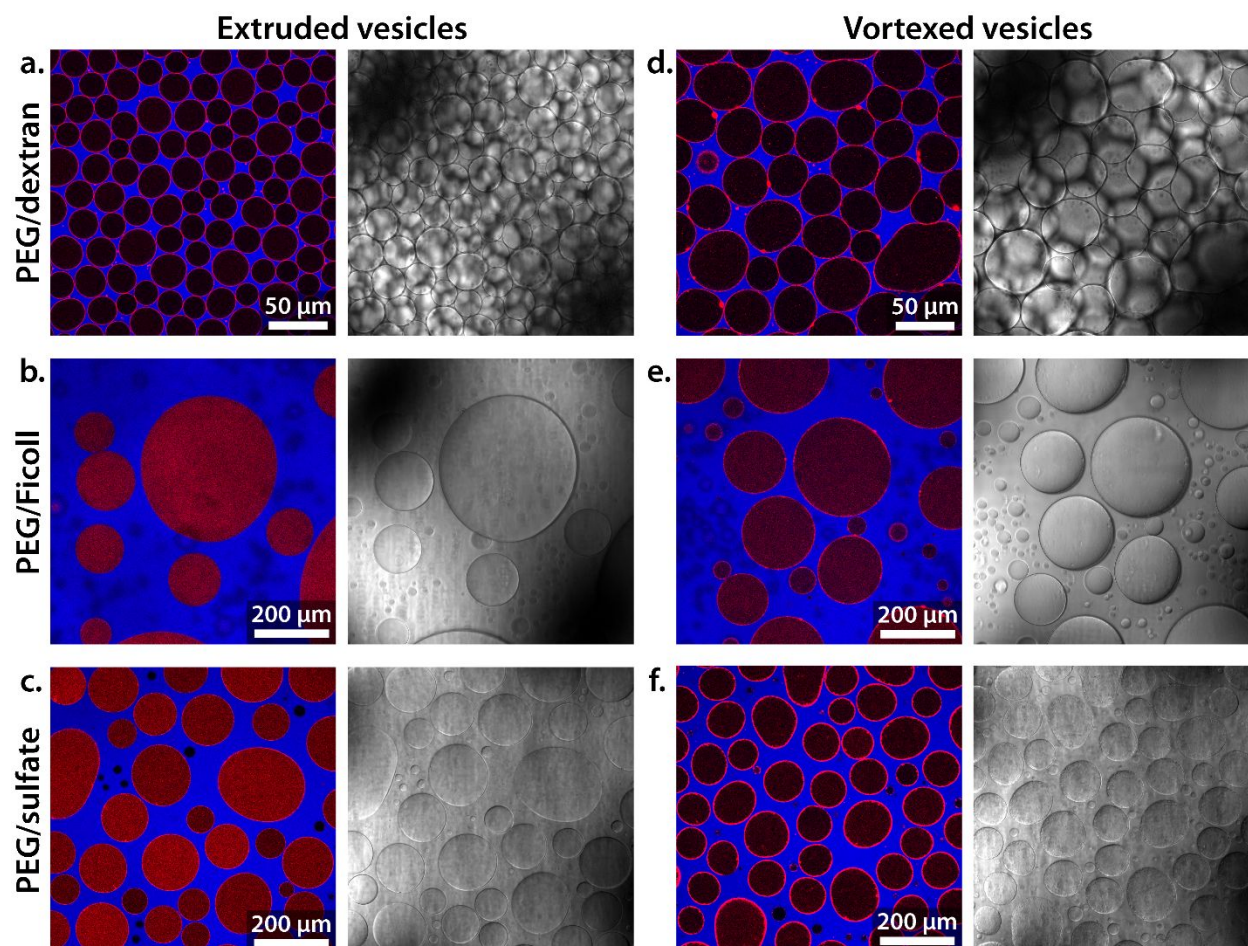


**Figure 3: Comparison of different vesicle-stabilized all-aqueous emulsions at 24 h.** Fluorescent confocal microscopy images of various aqueous two-phase separation (ATPS) emulsions stabilized with extruded (a, b, c) and vortexed (d, e, f) liposomes. 24 hours after initial sample preparation. Vortexed liposomes were able to effectively stabilize droplets of one phase within a continuous PEG-rich phase in the same manner as extruded liposomes with identical lipid composition. (a,d) PEG/dextran emulsions; (b,e) PEG/Ficoll emulsions; (c,f) PEG/sulfate emulsions. Left panels = overlaid fluorescence; right panels = brightfield. Rhodamine-tagged vesicles have been false colored red, Alexa 647-tagged PEG has been false colored blue.

### Vesicle distribution

The partitioning of extruded and vortexed vesicles in the different ATPS was investigated by measuring the relative fluorescence from Rhodamine-labeled vesicles in each phase (Table 1).

Although vesicles accumulated strongly at the aqueous/aqueous interface in all three ATPS systems tested here, some vesicles remained suspended in the phases as evidence by nonzero fluorescence intensity from labeled lipids. In all cases, the vesicles show at least slight preference for the dispersed phase over the continuous phase, with greater vesicle partitioning in the sulfate-rich dispersed phase of PEG/sulfate than the Ficoll-rich dispersed phase of Ficoll/PEG, and still weaker partitioning to the dextran-rich dispersed phase of the PEG/dextran system (Table 1). Vesicle partitioning into the dispersed phase increased over time, with a roughly twofold increase for extruded vesicles in any of the systems comparing 24 hr with initial samples (Table 1). The differences in vesicle partitioning between ATPS compositions are more noticeable in fluorescent line scans across the diameters the stabilized droplets (Figure 4, S3). The nature of the liposome assembles at the interface was investigated using the fluorescence recovery after photobleaching (FRAP) technique.<sup>45-46</sup> The diffusivity of the liposomes at the interface was determined by how quickly the fluorescent signal recovered at the bleached site. PEG/Dx ATPS emulsions were prepared using either extruded or vortexed vesicles, and part of the liposome lined interface was bleached (Figure S4). Regardless of whether the vesicles were extruded or not, the projected fits for the FRAP data suggest that the bleached portion will never fully recover. The lack of recovery indicates that not all of the liposomes are able to freely diffuse at the interface. Arrested in-plane diffusion could be the result of particle “jamming,” in which the high concentration of liposomes at the interface prevent free movement.<sup>47</sup>

**Table 1: Extruded and vortexed vesicle partitioning in the different ATPS tested.** Vesicle partitioning between the droplet and continuous phases was determined based on the relative fluorescent intensity (with background subtraction) of the Rhodamine-labeled vesicles in the two phases,  $(I_{\text{dispersed}} - I_{\text{background}})/(I_{\text{continuous PEG-rich}} - I_{\text{background}})$ . Uncertainty is the standard deviation of ~400 measurements.

ATPS composition (w/w)	Extruded vesicles, initial sample	Vortexed vesicles, initial sample	Extruded vesicles, 24 hours	Vortexed vesicles, 24 hours
10%/10% dextran/PEG	$1.8 \pm 0.4$	$1.3 \pm 0.2$	$5 \pm 2$	$4 \pm 1$
15%/10% Ficoll/PEG	$4.3 \pm 0.7$	$4.0 \pm 0.8$	$9 \pm 2$	$6 \pm 1$
8%/10% sulfate/PEG	$7 \pm 2$	$4 \pm 1$	$13 \pm 3$	$9 \pm 2$

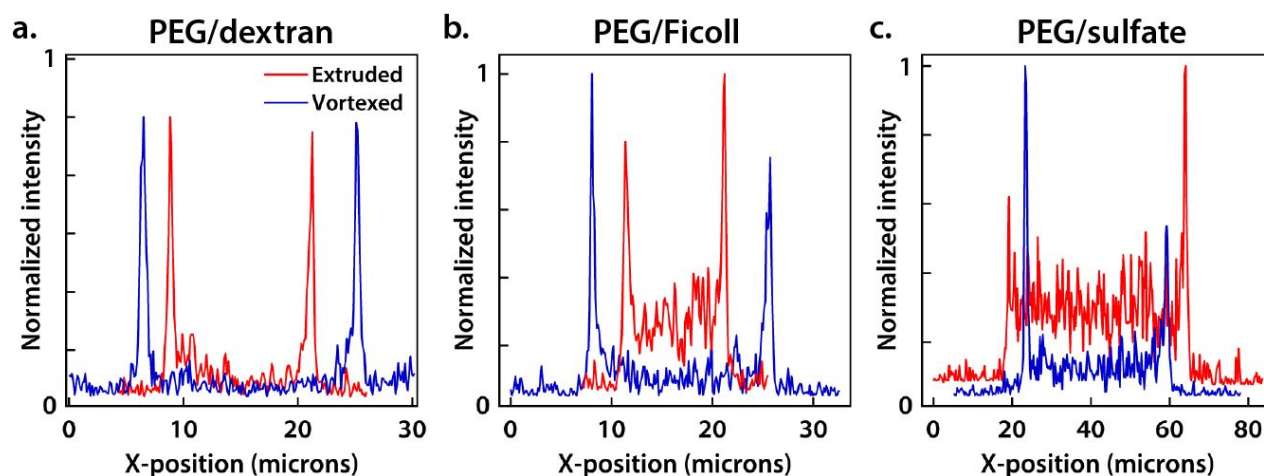


**Figure 4: Fluorescence intensity line scans of Rhodamine-labeled vesicle distribution in vesicle stabilized ATPS emulsions.** Line scans were performed across the full diameter of individual droplets in (a) PEG/dextran, (b) PEG/Ficoll, or (c) PEG/sulfate samples. X-axis refers to relative position along the diameter across the sample. Raw fluorescence data were extracted from fluorescent confocal microscopy images and normalized to their highest relative values.

### Permeability of the liposome-lined interface

The permeability of the liposome-coated interfaces was investigated by monitoring diffusion of a fluorescently labeled oligoRNA in these systems. Figure 5a depicts the reaction scheme used to qualitatively follow RNA diffusion in a quiescent sample. Externally added fluorescently labeled U15 freely diffuses through both the PEG and dextran-rich phases (Figure 5b). Over time, the RNA accumulates in the dextran-rich phase, in accordance with its



partitioning behavior (Table 2). The partitioning coefficients of RNA in these ATPS is consistent with previously reported values.<sup>44, 48</sup> Similar diffusion behavior can also be observed in emulsions prepared with PEG/Ficoll and PEG/sulfate ATPS (Figures S5, S6). In all cases, whether the vesicles were produced by extrusion or vortexing U15 can diffuse across the vesicle-coated interface into the dispersed phase droplets. Given the nature of local gradients in these experiments, however, relative rates of diffusion cannot be inferred.

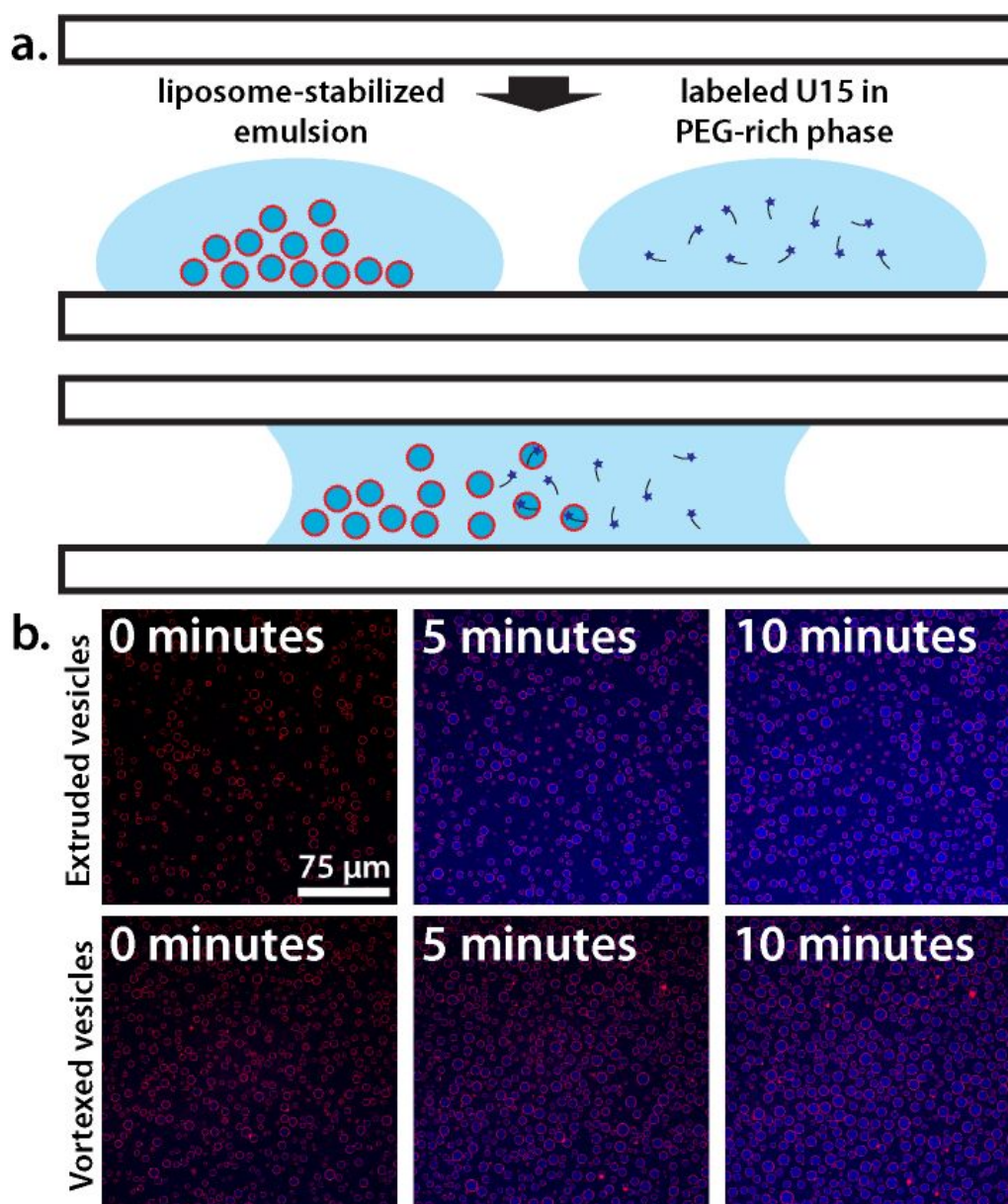


**Figure 5: Tracking the diffusion of fluorescently tagged U15 oligoRNA throughout stabilized emulsions.** (a) Experimental scheme used to monitor U15 diffusion through the liposome stabilized ATPS emulsion. Two droplets were placed adjacent on a glass slide functionalized with a PEG-silane: one containing a liposome stabilized ATPS emulsion, the other labeled U15 in PEG-rich phase. Contact between the two and subsequent U15 diffusion was initiated through the addition of a coverslip. (b) Fluorescent confocal microscopy images depicting diffusion of labeled-RNA (U15) through vesicle-stabilized PEG/dextran ATPS emulsions. Inset refers to time after diffusion initiation. Rhodamine-tagged vesicles have been false-colored red, Alexa 647-tagged U15 blue.

FRAP was used for a more quantitative comparison of U15 diffusion into liposome-stabilized dextran droplets. After bleaching an entire droplet, fluorescent U15 recovery was observed from the PEG-rich external phase into the dextran-rich droplet phase (Figure 6a). Figure 6b depicts normalized U15 fluorescence in the dextran-rich phase before and after bleaching in emulsions prepared with extruded and vortexed vesicles. In both cases, the dextran-rich phase fully recovered almost instantaneously. The half-time of recovery,  $\tau_{1/2}$ , for the dextran-rich phase was  $0.80 \pm 0.09$  seconds for the emulsion with extruded vesicles, and  $0.9 \pm 0.1$  seconds for the emulsion with vortexed vesicles. Emulsions prepared without any liposomes were not stable enough to allow for adequate FRAP analysis. Regardless of vesicle preparation technique, molecules were able to pass through the interface. This permeability is necessary for reactants to enter the dispersed, reactive phase.

**Table 2: OligoRNA (U15) partitioning in different ATPS emulsions with extruded vesicles, vortexed vesicles, or no vesicles present.** U15 partitioning was based on the relative Alexa-647 fluorescence in the two phases. Ratio is calculated as fluorescence intensity in the dispersed phase over intensity the PEG-rich phase. Uncertainty is the standard deviation of ~400 measurements.

ATPS composition (w/w)	No vesicles at interface	Extruded vesicles at interface	Vortexed vesicles at interface
10%/10% dextran/PEG	$1.82 \pm 0.09$	$2.2 \pm 0.3$	$1.9 \pm 0.2$
15%/10% Ficoll/PEG	$1.1 \pm 0.1$	$1.06 \pm 0.09$	$1.1 \pm 0.1$
8%/10% sulfate/PEG	$0.4 \pm 0.1$	$0.5 \pm 0.1$	$0.4 \pm 0.1$

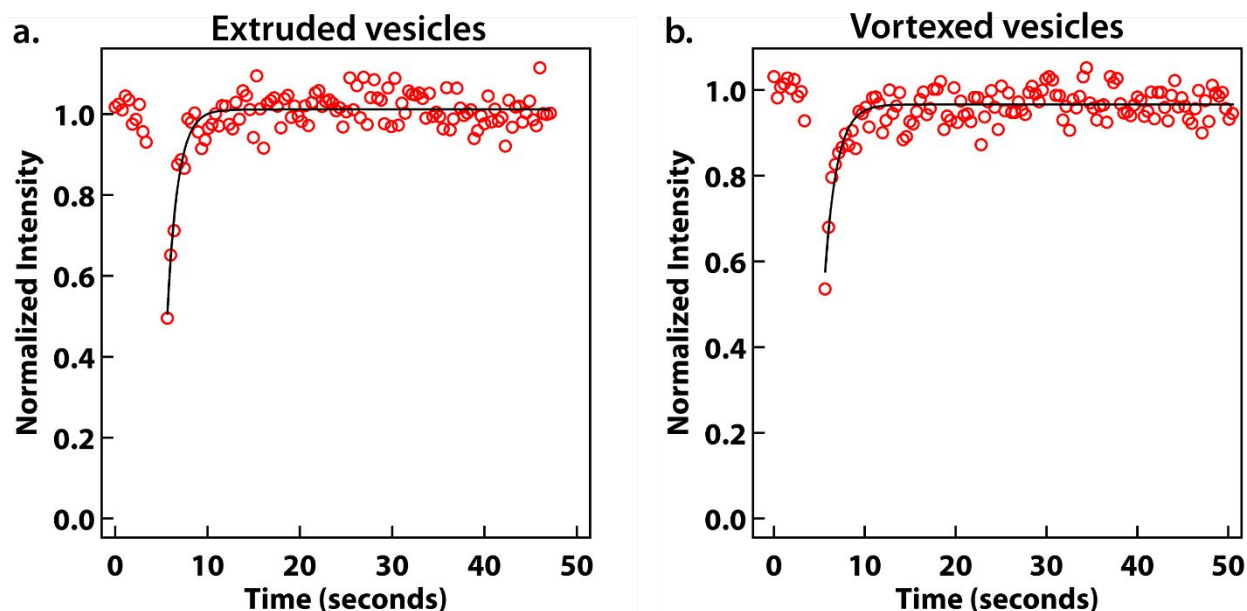


**Figure 6: Examining the interface permittivity of stabilized emulsions using FRAP.** Fluorescence recovery after photobleaching (FRAP) data for U15 diffusion in vesicle stabilized PEG/dextran ATPS emulsions prepared with (a) extruded and (b) vortexed vesicles. In-laid curves are data fits (Equation 1 in Methods).

### Encapsulating calcium carbonate synthesis

We previously reported urease-loaded, vesicle-stabilized PEG/Dx emulsions as artificial mineralization vesicles (AMVs).<sup>37</sup> Briefly, stabilized emulsions are loaded with urease and chelated  $\text{Ca}^{2+}$ . Urea added to the emulsion is hydrolyzed by urease to form carbonate, which then displaces the chelator to form  $\text{CaCO}_3$ . The enzyme reaction, and subsequent mineral formation, is localized to the dispersed phase based on urease partitioning selectively to the Dx-rich phase. In order to test whether AMVs prepared using vortexed rather than extruded lipid vesicles could still function as mineralizing microreactors, PEG/dextran-based AMVs were prepared using either extruded or vortexed vesicles. Figure 7 depicts AMVs before and after the addition of urea to the emulsion as imaged by darkfield microscopy. Prior to the addition of urea, only the diffraction of PEG/Dx interface can be observed in the images (Figure 7b). After the addition of urea (~40 minutes), bright spots due to light scattering from amorphous calcium carbonate begin to appear (Figure 7d). The observation of calcium carbonate particles indicates

successful encapsulation of the mineralization reaction in these AMVs. The reaction was also observed via confocal microscopy. The presence of mineral can be observed in the brightfield channel after the addition of urea to the system (Figure 7c, e).

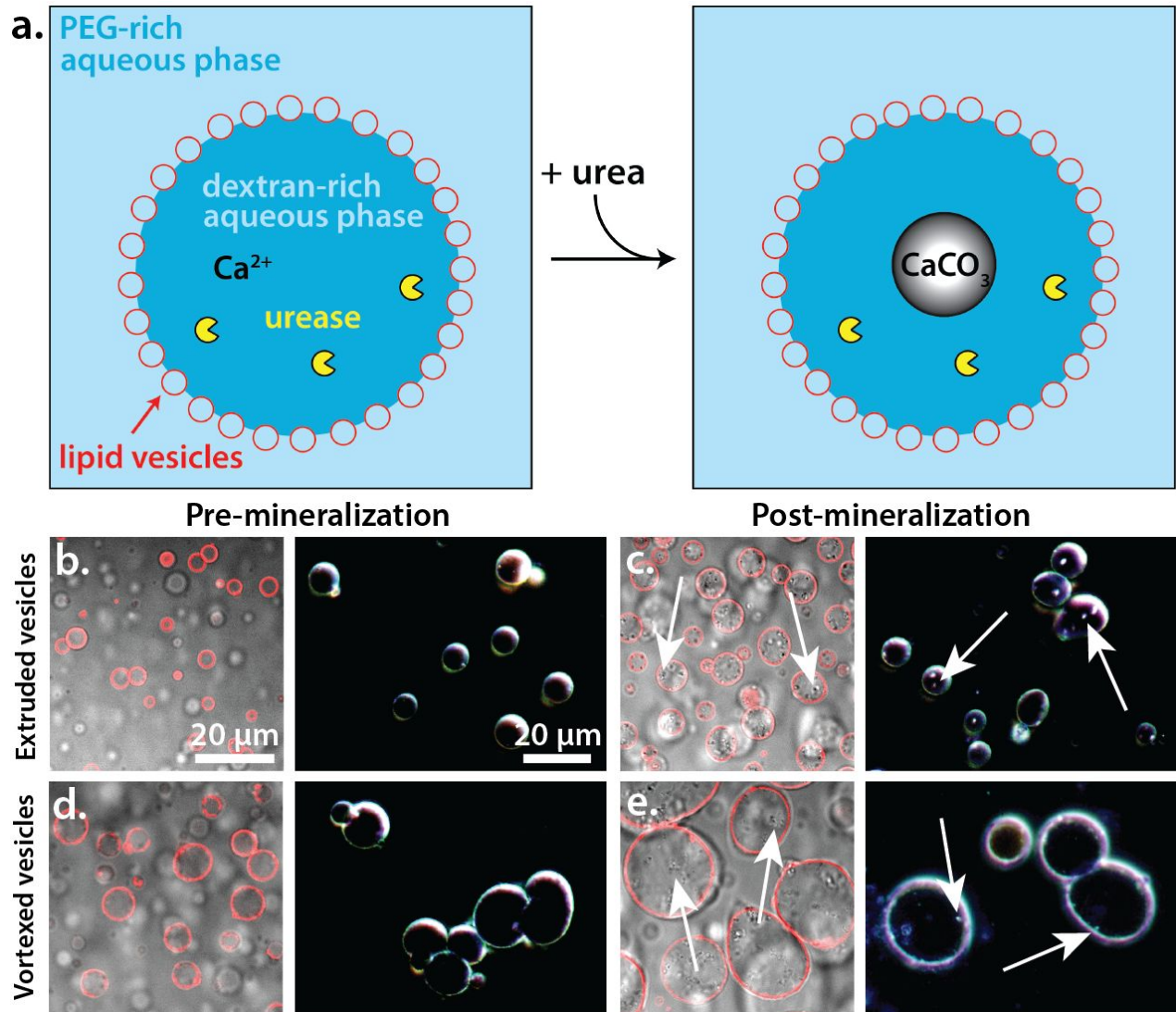


**Figure 7: Tracking  $\text{CaCO}_3$  formation inside vesicle-stabilized emulsions via confocal fluorescence and darkfield microscopy.** (a) Schematic depiction of  $\text{CaCO}_3$  formation inside artificial mineralization vesicles (AMVs.) (b-e) Microscopy images of AMVs stabilized with either (b, c) extruded or (d, e) vortexed liposomes. Left panels show confocal images and right panels show darkfield. (b, d) Before the addition of urea to the emulsion (pre-mineralization). (c, e) ~40 minutes after the addition urea to the emulsion (post-mineralization). Scale bars in (b) apply to all panels. Arrows denote the formed  $\text{CaCO}_3$ .



### Monitoring starch degradation in PEG/sulfate emulsions

An advantage of expanding the ATPS compositions that can be used in vesicle-stabilized all-aqueous emulsions is the possibility of choosing an ATPS based on its ability to selectively accumulate an enzyme of interest. For example, amylase displays greater partitioning behavior in the PEG/salt ATPS versus PEG/dextran.<sup>49, 50</sup> This enzyme selectively cleaves the 1,4-glycosidic linkage in starch, and has been used in several different industries, including textiles and detergents.<sup>51</sup> To test the viability of the vesicle-stabilized PEG/sulfate all-aqueous emulsion system for amylase-driven reactions, we monitored the degradation of starch by this enzyme. In these experiments we employ a starch substrate that is over-labeled with dye moieties to the point of self-quenching, such that amylase activity is indicated by increased fluorescence emission. Figure 8 depicts PEG/sulfate emulsions several minutes after the addition of over-labeled starch with or without  $\alpha$ -amylase present. In the presence of amylase, strong fluorescence signal is observed, particularly within the sulfate-rich droplets (Figure 8 a, c). This localization of fluorescent product within the sulfate-rich phase is presumably due to preferential partitioning of the product to this phase. Some background fluorescence can be seen in emulsions not containing enzyme, due to incomplete quenching and/or natural degradation in solution; this level is considerably lower than for the enzyme-containing samples (Figure 8 b, d). Systems using extruded or vortexed vesicles for emulsion stabilization behave essentially the same (compare Figure 8 panels a,b with c,d).

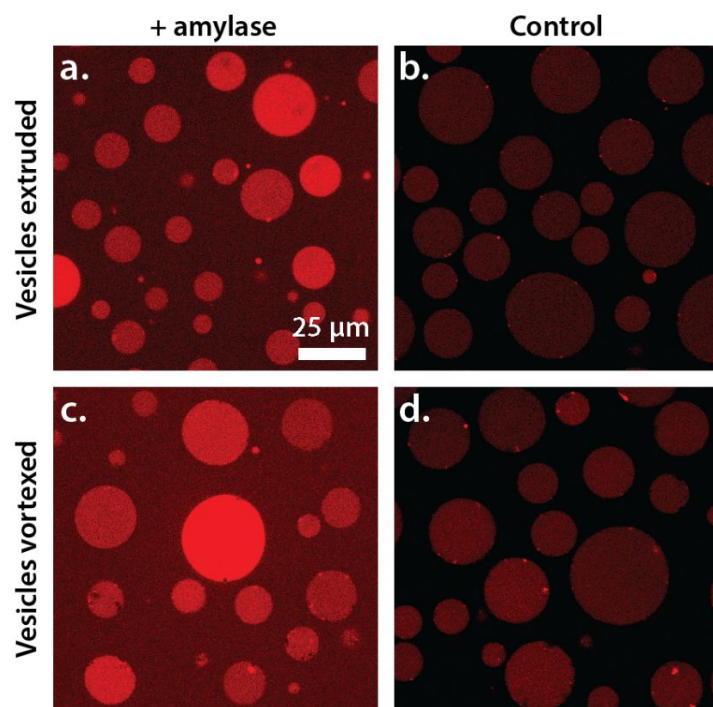


**Figure 8: Observing starch degradation inside vesicle-stabilized emulsions via confocal fluorescence microscopy.** Fluorescent confocal microscopy images of sulfate-rich droplets stabilized with either (a, b) extruded or (c, d) vortexed liposomes. Samples were prepared either (a, c) with or (b, d) without amylase, resulting in different degrees of starch degradation. All images were acquired ~30 minutes after sample formulation. Scale bar applies to all images.

## Discussion

The major outcome of this work is the generalization of vesicle-stabilized all-aqueous emulsion systems beyond the standard PEG/dextran + extruded vesicle system. We demonstrated that it was possible to substitute the simpler vortex method for extrusion to homogenize the lipid vesicles that are used to stabilize the emulsion droplets against coalescence. Size analysis demonstrated that extrusion resulted in smaller, more uniform vesicles than vortex mixing. These size distributions align with prior analyses of preparation methods, wherein extrusion produces vesicles with reduced lamellarity and radii.<sup>52</sup> The difference in vesicle size is reflected in the size distributions of the stabilized droplets. Smaller, more numerous vesicles can cover more surface area, resulting in smaller, stabilized droplets. Furthermore, it was

demonstrated that not only the traditional PEG/dextran but also PEG/Ficoll or PEG/sulfate ATPS can be used to form vesicle-stabilized all-aqueous emulsions. Although the PEG/dextran system produced smaller diameter, more uniform, and more stable droplet populations, all three systems produced suspensions of vesicle-coated droplets for which a model solute (fluorescently-labeled U15 RNA) added to the external continuous PEG-rich phase was able to enter the droplet interiors.

There were some differences between the three ATPS tested. Ficoll, a polymer of sucrose, is structurally similar to dextran, a polymer of glucose, and was anticipated to perform similarly. In contrast, PEG/sulfate was selected as a greater departure from the PEG/dextran system. Its salt-rich phase is physically and chemically quite dissimilar from the other interior phases, with nearly 1 M salt present,<sup>53</sup> and as such widens the choice of chemistries that could be performed in droplet interiors. Amylase, for instance, demonstrates stronger partitioning in the PEG/sulfate ATPS than the PEG/dextran ATPS.<sup>49, 50</sup> Inorganic salts such as sodium sulfate are also less expensive than purified polymers, which an important consideration for scaling up these reactors. The most obvious difference between the different ATPS compositions was the vesicle partitioning (Tables 1, Figure 4 and S3). The solubility of lipid vesicles in the two phases of each ATPS affects vesicle accumulation at the interface, in turn dictating the stability of the emulsion. Fewer vesicles at the surfaces means less total surface area that can be stabilized, meaning more coalescence can occur, giving rise to greater droplet sizes and broader droplet size distribution.

In general, extruded and vortexed liposomes appear to be similarly effective at stabilizing the emulsions and maintaining a permeable interface through which solutes such as U15 added to the exterior continuous phase can diffuse. Comparisons between vesicle preparation methods

showing greater similarity than comparisons between different ATPS compositions. An exception was seen for the PEG/sulfate system, where extrusion resulted in nearly a twofold increase in vesicle partitioning into the interior, salt-rich phase. The difference in partitioning may arise due to the difference in vesicle sizes, with the larger, vortexed vesicles having greater driving force for interfacial assembly.

The results presented here suggest that vesicle-stabilized all-aqueous emulsion systems are a general approach for preparing microscale bioreactors, with the composition of the ATPS and the preparation method of the vesicles tunable for a particular intended application. Since interfacial vesicle assembly is necessary for droplet stabilization, the choice of lipid headgroups is likely to be important. Here, the inclusion of both PEGylated and charged lipid headgroups facilitated interfacial vesicle accumulation.<sup>36</sup>

### **Acknowledgements**

This work was supported by the U.S. Department of Energy, Office of Science, Basic Energy Sciences under Award # DE-SC0008633.

### **Methods**

**Materials.** Calcium chloride dihydrate ( $\geq 99.5$  % purity), urea, poly(ethylene glycol) (PEG) 8 kDa, Ficoll® PM 70, urease from jack bean (*Canavalia ensiformis*) of activity 8.3 U/mg, and ethylenediamine-*N,N'*-disuccinic acid trisodium salt solution (EDDS)(~35% in H<sub>2</sub>O) was purchased from Sigma-Aldrich, Co. (St. Louis, MO). Dextran (Dx) 10 kDa was purchased from Toronto Research Chemicals, Inc. (Toronto, Canada). Methyl-PEG-amine 8 kDa was purchased

from Nektar Therapeutics (San Francisco, CA). Alexa 647 carboxylic acid, succinimidyl ester and EnzChek *Ultra* amylase assay kit was purchased from ThermoFisher (Waltham, MA). The amylase assay kit contained DQ starch from corn, BODIPY FL conjugate and 50 mM sodium acetate (pH 4.0). Egg-phosphatidylcholine (Egg-PC), egg-phosphatidylglycerol (Egg-PG), 1, 2-dioleoyl-*sn*-glycero-3-phosphoethanolamine-poly(ethylene glycol) 2 kDa (DOPE-PEG 2 kDa), and 1,2-dioleoyl-*sn*-glycero-3-phosphoethanolamine-N-(lissamine rhodamine B sulfonyl) (Rh-DOPE) lipids were purchased from Avanti Polar Lipids, Inc. (Alabaster, AL). Alexa-647 tagged U15 was custom ordered from Integrated DNA Technologies, Inc. (Coralville, IA). Bio-Gel P-6 gel was purchased from Bio Rad Laboratories (Hercules, CA). Amylase of activity 50 U/mg was purchased from VWR (Radnor, PA). Fluorescently tagged PEG was prepared in house by reacting Alexa 647 carboxylic acid, succinimidyl ester with methyl-PEG-amine. Briefly, the polymer and the reactive label were mixed for 1 hour and excess label was removed using a size exclusion column loaded with Bio-Gel P-6 gel.

**Formation of aqueous two-phase separations (ATPS).** A 10 g stock ATPS was made by dissolving 1 g PEG 8 kDa and 1 g Dx 10 kDa in 8 g 10 mM pH 7.4 Tris buffer, for a final formulation of 10%/10% w/w PEG 8 kDa/Dx 10 kDa. Identical preparation methods were used to make 10 g stock ATPS with final formulations of 10%/15% w/w PEG 8 kDa/Ficoll 70 kDa and 10%/8% w/w PEG 8 kDa/sulfate. The mixtures were stirred in 15 mL centrifuge tubes for 1 hour to dissolve the polymers. The PEG/Dx and PEG/Ficoll ATPS sat at 5°C and phase separate overnight, while the PEG/sulfate ATPS sat at 25°C. The individual phases were then carefully removed via pipet and stored in separate tubes at 5°C. All phases were disposed of one week after separation.

**Formation of liposomes.** All vesicles were initially prepared using the gentle hydration method. Phospholipids dissolved in chloroform were pooled in the bottom of borosilicate glass tubes with the following composition: 48.5 mol% Egg PC; 48.5 mol% Egg PG; 2.8 mol% DOPE-PEG-2kDa; 0.1 mol% Rh-DOPE. Lipids were dried under a gentle stream of argon (~5 psi) then under vacuum for 1 hour. Films were then hydrated with PEG-rich from a separated 10%/10% w/w PEG/dextran ATPS, PEG-rich phase from a separated 10%/15% PEG/Ficoll ATPS, or a 25% w/w PEG solution for a lipid concentration of 7.5 mg/mL. After incubating the thin films at 40°C for 72 hours, liposomes received one of two treatment methods, hereto referred to as extruded and vortexed. Extruded vesicles were passed through an Avanti Polar Lipids Mini Extruder lined with 100 nm membranes 11 times total. Vortexed vesicles were placed on a vortex mixer at maximum velocity for ~10 seconds and used without further treatment. Both extruded and vortexed vesicles were stored at 5°C prior to use and disposed of after one week.

**Dynamic light scattering.** 1 mL samples were prepared by diluting 30 µL of vesicle stock solution hydrated with PEG-rich phase from PEG/Dx ATPS, extruded or vortexed in 970 µL of isotonic fructose solution (183 mmol/kg). Average vesicle diameter was measured using dynamic light scattering analysis on the Malvern Zetasizer. 1 mL of undiluted gentle hydration raw product, hydrated with PEG-rich from PEG/Dx ATPS, was also analyzed.

**Droplet size analysis and fluorescence partitioning.** 20 µL emulsions were prepared by mixing 2 µL 7.5 mg/mL liposome stock solution, 16 µL separated PEG-rich phase, and 2 µL separated Dx-rich phase, for a final composition of 10% by volume vesicles and 1:9 Dx:PEG

volume ratio. Samples used in time studies were also loaded with 50  $\mu\text{g}/\text{mL}$  ampicillin to inhibit any bacterial growth. Samples were mixed on the vortex mixer for  $\sim 3$  minutes immediately prior to analysis. Identical volumes were used to create the stabilized PEG/Ficoll and PEG/sulfate ATPS emulsions. Both extruded and vortexed liposomes were used at equal concentrations. For partitioning and size analysis, 20  $\mu\text{L}$  of sample was deposited on a silanized glass slide with silanized coverslip, separated by a 160  $\mu\text{m}$  silicone spacer. Samples analyzed again after 24 hours were left on their slides and placed adjacent to 50 mL beaker of water under a large petri dish to prevent drying out. All samples were imaged on a Leica (Wetzlar, Germany) TCS SP5 PL confocal microscope using a 63x 1.4 NA APO objective or a 20x 0.7 NA APO objective.

**U15 diffusion.** 200  $\mu\text{L}$  emulsions were prepared by mixing 5  $\mu\text{L}$  7.5 mg/mL liposome stock solution, 189  $\mu\text{L}$  separated PEG-rich phase, and 6  $\mu\text{L}$  separated Dx-rich phase, for a final composition of 2.5% by volume vesicles and 1:97 Dx:PEG volume ratio. Identical volumes were used to create the stabilized PEG/Ficoll and PEG/sulfate ATPS emulsions. Both extruded and vortexed liposomes were used at equal concentrations. 20  $\mu\text{L}$  of the emulsion was deposited adjacent to 20  $\mu\text{L}$  PEG-rich phase loaded with 0.5  $\mu\text{M}$  Alexa 647-tagged U15 on a silanized glass slide with 160  $\mu\text{m}$  silicone spacer. Contact between the two droplets was initiated by the addition of a silanized cover-slip. Fluorescent images of the stabilized emulsions were acquired over the course of U15 diffusion on the confocal microscope. For each experiment, two regions of interest (ROI's) within the emulsion were selected: one inside an arbitrarily selected droplet of dispersed phase, one in the adjacent continuous phase. The ROIs would move in each image in order to account for sample drift while still allowing for the most accurate comparison between

the two phases. Average fluorescent intensity in both ROIs over the course of diffusion was measured using ImageJ software.

**Fluorescence recovery after photobleaching.** 20  $\mu\text{L}$  emulsions were prepared by mixing 2  $\mu\text{L}$  7.5 mg/mL liposome stock solution, 17  $\mu\text{L}$  separated PEG-rich phase, and 1  $\mu\text{L}$  separated Dx-rich phase, for a final composition of 10% by volume vesicles and 1:19 Dx:PEG volume ratio. Samples were also equilibrated with 0.5  $\mu\text{M}$  Alexa Fluor 647-labeled poly U15. FRAP studies were performed with an excitation of 633 nm for the labeled poly U15. After selecting a stabilized dextran-rich phase droplet for analysis, a 10-frame prebleach sequence followed a 5-frame bleach at 100% 458, 476, 488, 514, 543, and 633 nm laser power for labeled poly U15. The entire droplet, as well as some of the surrounding continuous PEG-rich phase, was bleached with a square region of interest (ROI). Recovery was measured by tracking the fluorescent intensity during the postbleach sequence, using a circular ROI, 2 micron in diameter, confined to the droplet interior during the pre- and postbleach sequences. Different sized ROI's were used for bleaching and measurements to account for sample drift throughout the experiment. For all FRAP experiments, the fluorescent noise was measured using 2 micron diameter circle as a background ROI with all lasers turned off and respective photomultiplier tubes (PMTs) turned on. Recovery data was normalized as described by Phiar et al. through the double normalization method.<sup>29</sup> The normalized data were then fit with a single exponential expression:

$$(1) \quad y = y_0 + Ae^{\frac{-(x-x_0)}{\tau}}$$

**Imaging  $\text{CaCO}_3$  synthesis on the darkfield microscope.** An adapted version of the previously reported artificial mineralization vesicle method was used. Relative liposome volumes were changed to create better imaging conditions. A 100  $\mu\text{L}$  ATPS with 10 vol. % extruded vesicles



or 10 vol. % vortexed vesicles of  $V_{\text{Dex}} : V_{\text{PEG}} 1 : 49$  was formulated, with 12.45 units/mL urease, 25 mM  $\text{Ca}^{2+}$  and 30 mM EDDS, and emulsified using a vortex mixer immediately prior to analysis. To maintain the ATPS volume ratio, all stock solutions were prepared in PEG-rich phase. 50  $\mu\text{L}$  of the emulsion was deposited on a silanized glass slide with no cover slip. The sample was then transferred to the microscope sample stage. To initiate the reaction, 5 M urea in PEG-rich phase was added to the emulsion for a final concentration of 100 mM urea, and a silanized glass coverslip was placed on top. Darkfield images were acquired periodically over the course of the reaction using an Olympus BX51 with darkfield illumination and a 100x objective.

**Imaging  $\text{CaCO}_3$  synthesis on the confocal microscope.** An adapted version of the previously reported artificial mineralization vesicle method was used. Relative liposome volumes and calcium concentrations were changed to create better imaging conditions. A 100  $\mu\text{L}$  ATPS with 10 vol. % extruded vesicles or 10 vol. % vortexed vesicles of  $V_{\text{Dex}} : V_{\text{PEG}} 1 : 49$  was formulated, with 12.45 units/mL urease, 30 mM  $\text{Ca}^{2+}$  and 25 mM EDDS, and emulsified using a vortex mixer immediately prior to analysis. To maintain the ATPS volume ratio, all stock solutions were prepared in PEG-rich phase. 50  $\mu\text{L}$  of the emulsion was deposited on a silanized glass slide with no cover slip. The sample was then transferred to the microscope sample stage. To initiate the reaction, 5 M urea in PEG-rich phase was added to the emulsion for a final concentration of 100 mM urea, and a silanized glass coverslip was placed on top. Fluorescent confocal images were acquired periodically over the course of the reaction using a Leica (Wetzlar, Germany) TCS SP5 PL confocal microscope using a 63x 1.4 NA APO objective.

**Imaging starch degradation on the confocal microscope.** A 100  $\mu\text{L}$  ATPS with 10 vol. % extruded vesicles or 10 vol. % vortexed vesicles of  $V_{\text{sulfate}} : V_{\text{PEG}} 1 : 9$  was formulated, with or without 0.5 units/mL  $\alpha$ -amylase. To maintain the ATPS volume ratio, all stock solutions were prepared in PEG-rich phase (or PEG solution, in the case of vesicles.) 1  $\mu\text{L}$  of 1 mg/mL starch BODIPY conjugate in 50 mM sodium acetate (pH 4.0) was equilibrated with each formulated emulsion. 10  $\mu\text{L}$  of each emulsion was deposited on a silanized glass slide with spacer and coverslip. Fluorescent confocal images of each sample were acquired periodically over the course of the reaction using a Leica (Wetzlar, Germany) TCS SP5 PL confocal microscope using a 63x 1.4 NA APO objective.

## References

1. Douliez, J. P.; Perro, A.; Beven, L., Stabilization of All-in-Water Emulsions To Form Capsules as Artificial Cells. *ChemBioChem* **2019**, *20* (20), 2546-2552.
2. Deng, N. N.; Yelleswarapu, M.; Zheng, L. F.; Huck, W. T. S., Microfluidic Assembly of Monodisperse Vesosomes as Artificial Cell Models. *J. Am. Chem. Soc.* **2017**, *139* (2), 587-590.
3. Liu, L. B.; Xiang, N.; Ni, Z. H., Droplet-based microreactor for the production of micro/nano-materials. *Electrophoresis*, 19.
4. Wei, L. J.; Zhang, M.; Zhang, X. M.; Xin, H. C.; Yang, H. Q., Pickering Emulsion as an Efficient Platform for Enzymatic Reactions without Stirring. *ACS Sustain. Chem. Eng.* **2016**, *4* (12), 6838-6843.
5. Xie, C. Y.; Meng, S. X.; Xue, L. H.; Bai, R. X.; Yang, X.; Wang, Y. L.; Qiu, Z. P.; Binks, B. P.; Guo, T.; Meng, T., Light and Magnetic Dual-Responsive Pickering Emulsion Micro Reactors. *Langmuir* **2017**, *33* (49), 14139-14148.
6. Liu, Z. N.; Wang, B. D.; Jin, S. H.; Wang, Z. D.; Wang, L.; Liang, S., Bioinspired Dual-Enzyme Colloidosome Reactors for High-Performance Biphasic Catalysis. *ACS Appl. Mater. Interfaces* **2018**, *10* (48), 41504-41511.
7. de Jong, H. G. B.; Kruyt, H. R., Coacervation (Partial miscibility on colloid systems) (Preliminary communication). *Proc. K. Akad. Wet.-Amsterdam* **1929**, *32* (6/10), 849-856.
8. Priftis, D.; Tirrell, M., Phase behaviour and complex coacervation of aqueous polypeptide solutions. *Soft Matter* **2012**, *8* (36), 9396-9405.
9. Sing, C. E.; Perry, S. L., Recent progress in the science of complex coacervation. *Soft Matter* **2020**, *16* (12), 2885-2914.
10. Crosby, J.; Treadwell, T.; Hammerton, M.; Vasilakis, K.; Crump, M. P.; Williams, D. S.; Mann, S., Stabilization and enhanced reactivity of actinorhodin polyketide synthase minimal complex in polymer-nucleotide coacervate droplets. *Chem. Commun.* **2012**, *48* (97), 11832-11834.
11. Koga, S.; Williams, D. S.; Perriman, A. W.; Mann, S., Peptide-nucleotide microdroplets as a step towards a membrane-free protocell model. *Nat. Chem.* **2011**, *3* (9), 720-724.

12. Li, J. B.; Liu, X. M.; Abdelmohsen, L.; Williams, D. S.; Huang, X., Spatial Organization in Proteinaceous Membrane-Stabilized Coacervate Protocells. *Small* **2019**, *15* (36), 9.
13. Brooks, D. E.; Sharp, K. A.; Fisher, D., 2 - Theoretical Aspects of Partitioning. In *Partitioning in Aqueous Two-Phase System*, Walter, H.; Brooks, D. E.; Fisher, D., Eds. Academic Press: 1985; pp 11-84.
14. Huddleston, J.; Veide, A.; Kohler, K.; Flanagan, J.; Enfors, S. O.; Lyddiatt, A., The molecular-basis of partitioning in aqueous 2-phase systems. *Trends Biotechnol.* **1991**, *9* (11), 381-388.
15. Huddleston, J. G.; Willauer, H. D.; Griffin, S. J.; Rogers, R. D., Aqueous polymeric solutions as environmentally benign liquid liquid extraction media. *Ind. Eng. Chem. Res.* **1999**, *38* (7), 2523-2539.
16. Iqbal, M.; Tao, Y. F.; Xie, S. Y.; Zhu, Y. F.; Chen, D. M.; Wang, X.; Huang, L. L.; Peng, D. P.; Sattar, A.; Shabbir, M. A.; Hussain, H. I.; Ahmed, S.; Yuan, Z. H., Aqueous two-phase system (ATPS): an overview and advances in its applications. *Biol. Proced. Online* **2016**, *18*, 18.
17. Shibata, C.; Iwashita, K.; Shiraki, K., Selective separation method of aggregates from IgG solution by aqueous two-phase system. *Protein Expr. Purif.* **2019**, *161*, 57-62.
18. Cans, A. S.; Andes-Koback, M.; Keating, C. D., Positioning lipid membrane domains in giant vesicles by micro-organization of aqueous cytoplasm mimic. *J. Am. Chem. Soc.* **2008**, *130* (23), 7400-7406.
19. Long, M. S.; Cans, A. S.; Keating, C. D., Budding and asymmetric protein microcompartmentation in giant vesicles containing two aqueous phases. *J. Am. Chem. Soc.* **2008**, *130* (2), 756-762.
20. Long, M. S.; Jones, C. D.; Helfrich, M. R.; Mangeney-Slavin, L. K.; Keating, C. D., Dynamic microcompartmentation in synthetic cells. *Proc. Natl. Acad. Sci. U. S. A.* **2005**, *102* (17), 5920-5925.
21. Dimova, R.; Lipowsky, R., Lipid membranes in contact with aqueous phases of polymer solutions. *Soft Matter* **2012**, *8* (24), 6409-6415.
22. Crowe, C. D.; Keating, C. D., Liquid-liquid phase separation in artificial cells. *Interface Focus* **2018**, *8* (5), 17.
23. Ellis, R. J., Macromolecular crowding: obvious but underappreciated. *Trends Biochem.Sci.* **2001**, *26* (10), 597-604.
24. Dix, J. A.; Verkman, A. S., Crowding effects on diffusion in solutions and cells. In *Annual Review of Biophysics*, Annual Reviews: Palo Alto, 2008; Vol. 37, pp 247-263.
25. Albertsson, P. A., Partition of cell particles and macromolecules in polymer two-phase systems. *Advances in protein chemistry* **1970**, *24*, 309-41.
26. Baskir, J. N.; Hatton, T. A.; Suter, U. W., Protein partitioning in 2-phase aqueous polymer systems. *Biotechnol. Bioeng.* **1989**, *34* (4), 541-558.
27. Chevalier, Y.; Bolzinger, M. A., Emulsions stabilized with solid nanoparticles: Pickering emulsions. *Colloid Surf. A-Physicochem. Eng. Asp.* **2013**, *439*, 23-34.
28. Dickinson, E., Particle-based stabilization of water-in-water emulsions containing mixed biopolymers. *Trends Food Sci. Technol.* **2019**, *83*, 31-40.
29. Chatsivili, N.; Philipse, A. P.; Loppinet, B.; Tromp, R. H., Colloidal zein particles at water-water interfaces. *Food Hydrocolloids* **2017**, *65*, 17-23.
30. de Freitas, R. A.; Nicolai, T.; Chassenieux, C.; Benyahia, L., Stabilization of Water-in-Water Emulsions by Polysaccharide-Coated Protein Particles. *Langmuir* **2016**, *32* (5), 1227-1232.
31. Binks, B. P.; Shi, H., Phase Inversion of Silica Particle-Stabilized Water-in-Water Emulsions. *Langmuir* **2019**, *35* (11), 4046-4057.
32. Peddireddy, K. R.; Nicolai, T.; Benyahia, L.; Capron, I., Stabilization of Water-in-Water Emulsions by Nanorods. *ACS Macro Lett.* **2016**, *5* (3), 283-286.
33. Ben Ayed, E.; Cochereau, R.; Dechance, C.; Capron, I.; Nicolai, T.; Benyahia, L., Water-In-Water Emulsion Gels Stabilized by Cellulose Nanocrystals. *Langmuir* **2018**, *34* (23), 6887-6893.

34. Hann, S. D.; Niepa, T. H. R.; Stebe, K. J.; Lee, D., One-Step Generation of Cell-Encapsulating Compartments via Polyelectrolyte Complexation in an Aqueous Two Phase System. *ACS Appl. Mater. Interfaces* **2016**, *8* (38), 25603-25611.
35. Hann, S. D.; Stebe, K. J.; Lee, D., AWE-somes: All Water Emulsion Bodies with Permeable Shells and Selective Compartments. *ACS Appl. Mater. Interfaces* **2017**, *9* (29), 25023-25028.
36. Dewey, D. C.; Strulson, C. A.; Cacace, D. N.; Bevilacqua, P. C.; Keating, C. D., Bioreactor droplets from liposome-stabilized all-aqueous emulsions. *Nat. Commun.* **2014**, *5*, 9.
37. Cacace, D. N.; Rowland, A. T.; Stapleton, J. J.; Dewey, D. C.; Keating, C. D., Aqueous Emulsion Droplets Stabilized by Lipid Vesicles as Microcompartments for Biomimetic Mineralization. *Langmuir* **2015**, *31* (41), 11329-11338.
38. Rowland, A. T.; Cacace, D. N.; Pulati, N.; Gulley, M. L.; Keating, C. D., Bioinspired Mineralizing Microenvironments Generated by Liquid-Liquid Phase Coexistence. *Chemistry of Materials* **2019**, *31* (24), 10243-10255.
39. Novak, U.; Lakner, M.; Plazl, I.; Znidarsic-Plazl, P., Experimental studies and modeling of alpha-amylase aqueous two-phase extraction within a microfluidic device. *Microfluid. Nanofluid.* **2015**, *19* (1), 75-83.
40. Vobecka, L.; Romanov, A.; Slouka, Z.; Hasal, P.; Pribyl, M., Optimization of aqueous two-phase systems for the production of 6-aminopenicillanic acid in integrated microfluidic reactors-separators. *New Biotech.* **2018**, *47*, 73-79.
41. Aumiller, W. M.; Davis, B. W.; Hatzakis, E.; Keating, C. D., Interactions of Macromolecular Crowding Agents and Cosolutes with, Small-Molecule Substrates: Effect on Horseradish Peroxidase Activity with Two Different Substrates. *J. Phys. Chem. B* **2014**, *118* (36), 10624-10632.
42. Rodriguez, N.; Pincet, F.; Cribier, S., Giant Vesicles formed by gentle hydration and electroformation: A comparison by fluorescence microscopy. *Colloids Surf. B* **2005**, *42* (2), 125-130.
43. Kikuchi, H.; Suzuki, N.; Ebihara, K.; Morita, H.; Ishii, Y.; Kikuchi, A.; Sugaya, S.; Serikawa, T.; Tanaka, K., Gene delivery using liposome technology. *J. Control. Release* **1999**, *62* (1-2), 269-277.
44. Strulson, C. A.; Molden, R. C.; Keating, C. D.; Bevilacqua, P. C., RNA catalysis through compartmentalization. *Nat. Chem.* **2012**, *4* (11), 941-946.
45. Phair, R. D.; Gorski, S. A.; Misteli, T., Measurement of dynamic protein binding to chromatin in vivo, using photobleaching microscopy. *Methods Enzymol.* **2004**, *375*, 393-414.
46. Pincet, F.; Adrien, V.; Yang, R.; Delacotte, J.; Rothman, J. E.; Urbach, W.; Tareste, D., FRAP to Characterize Molecular Diffusion and Interaction in Various Membrane Environments. *PLoS One* **2016**, *11* (7), 19.
47. Pawar, A. B.; Caggioni, M.; Ergun, R.; Hartel, R. W.; Spicer, P. T., Arrested coalescence in Pickering emulsions. *Soft Matter* **2011**, *7* (17), 7710-7716.
48. Jia, T. Z.; Hentrich, C.; Szostak, J. W., Rapid RNA Exchange in Aqueous Two-Phase System and Coacervate Droplets. *Orig. Life Evol. Biosph.* **2014**, *44* (1), 1-12.
49. Schmidt, A. S.; Ventom, A. M.; Asenjo, J. A., Partitioning and purification of  $\alpha$ -amylase in aqueous two-phase systems. *Enzyme Microb. Technol.* **1994**, *16* (2), 131-142
50. Li, M.; Kim, J-W.; Peeples, T. L., Amylase partitioning and extractive bioconversion of starch using thermoseparating aqueous two-phase systems. *J. Biotechnol.* **2002**, *93* (1), 15-26
51. Michelin, M.; Silva, T. M.; Benassi, V. M.; Peixoto-Nogueira, S. C.; Moraes, L. A. B.; Leão, J. M.; Jorge, J. A.; Terenzi, H. F.; Polizi, M. L. T. M., Purification and characterization of a thermostable  $\alpha$ -amylase produced by the fungus *Paecilomyces variotii*. *Carbohydr. Res.* **2010**, *345* (16), 2348-2353.
52. Olson, F.; Hunt, C. A.; Szoka, F. C.; Vail, W. J.; Padahadjopoulos, D., Preparation of liposomes of defined size distribution by extrusion through polycarbonate membranes. *Biochim. Biophys. Acta* **1979**, *557* (1), 9-23

53. Ferreira, L. A.; Teixeira, J. A., Salt Effect on the Aqueous Two-Phase System PEG 8000-Sodium Sulfate. *J. Chem. Eng. Data* **2011**, *56* (1), 133-137.